23rd ABCM International Congress of Mechanical Engineering
December 6-11, 2015, Rio de Janeiro, RJ, Brazil

FLOW ANALYSIS THROUGH AN ARTERIOVENOUS FISTULA OBTAINED FROM COMPUTED TOMOGRAPHY

Fábio César Miranda de Oliveira
Kleiber Lima de Bessa
José Ubiragi Mendes de Lima
Federal University of Rio Grande do Norte. Department of Mechanical Engineering, Center of Technology, Avenida Senador Salgado Filho, 300 – Lagoa Nova, CEP 59078-970 – Natal/RN
fah_hc@hotmail.com
klbessa@ct.ufrn.br
ubiragi@ct.ufrn.br

Ricardo Wagner da Costa Moreira
Federal University of Rio Grande do Norte. Department of Integrated Medicine, Center for Health Sciences, Avenida Nilo Pecanha, s/n – Petrópolis, CEP 59012-300 – Natal/RN
ricardowagnermoreira@gmail.com

Abstract. *The purpose of these instructions is to serve as a guide for formatting papers to be published in the Proceedings of the XXII COBEM. The abstract should describe the objectives, the methodology and the main conclusions of the paper in about 200 words. It should contain neither formulae nor reference to bibliography. The abstract will be included in a printed volume to be distributed to the symposium participants, whilst the full paper will be published in the proceedings.*

Keywords: fístula, CFD, recirculation, wall shear stress

1. INTRODUCTION

The vascular access for hemodialysis patients usually is through native arteriovenous fistula (AVF) or synthetic grafts to allow adequate blood flow during the dialysis session (Yerdel et al., 1997). The preferred vascular accesses is AVF because that shows lower infection rates. Creation of an AVF entails a dramatic change in local hemodymanic conditions in the vicinity of the fistula. The maturation is an active process of vascular remodeling that is a response to the altered biomechanical forces induced in the vascular system by placement of the fistula. After creating the AVF, blood flow rate slowly progresses and reaches an average of 1200 ml min-1 after maturation (Wedgwood et al., 1984). After or during the maturation process, experimental and numerical evidence for recirculation, low and high wall shear stress (WSS), and turbulent hemodynamic can generate some pathologys. Common complications are formation of stenosis, thrombosis, aneurysms (Van et al., 2005) and intimal hyperplasia (Sivanesan et al., 1999).

Developing an understanding of the relationship between the blood flow and hemodynamic complications requires accurate measurements of physiological parameters and a detailed 3D analysis of the local blood flow pattern. According to exposed, this study used the computational fluid dynamic (CFD) associated with computed tomography (CT) to modeling and analysis the flow patterns and wall shear stress in AVF. The pulsatile flow simulated was obtained from Sivanesan et al. (1999) entitled: Flow patterns in the radiocephalic arteriovenous fistula: an in vitro study. Thus, the aim of this paper is understand a little bit the relation between flow patterns and vascular complications in the arteriovenous fistula.

2. METHODS

The studied patient is male, 72 years old and has an end-lateral fistula on the left arm venous aneurysm. For these simulations the blood was considered Newtonian incompressible and homogeneous.

2.1 Geometric model

Using public software InVesalius 3.0 geometry was built using 1000 CT images. A polygonal surface made of triangles was generate (Figure 1). The aneurism and anastomosis have a diameter of approximately 16mm and 10mm, respectively. Only the surface of interest has been exported in STL format for the mesh generator. Due to considerable amount of collagen fibers in the region, all the walls of the vessels were considered rigid.

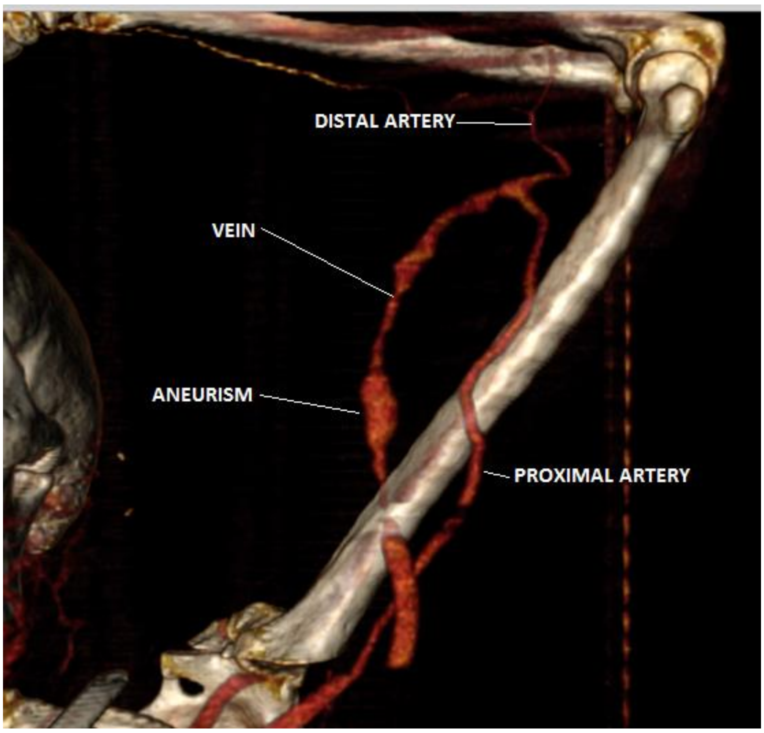

Figure 1. Geometry generated

2.2 Mesh

A three-dimensional mesh was built in the AVF. The software used was ANSYS ICEM 13 (Academic License). The mesh has tetrahedral format in the inner regions of the blood vessels, prismatic near to the walls and triangular in the surface. The size of the volume elements become increasingly smaller in nearby regions of the walls due to higher gradients are located, the growth of a rule elements obeyed exponential.

The total of the volume elements was 11346. The minimum quality used for volumetric elements was 0.4 (Figure 2). The mesh was refined until the flow parameters did not change any further, or rather the results presented in this investigation are meshing independent.

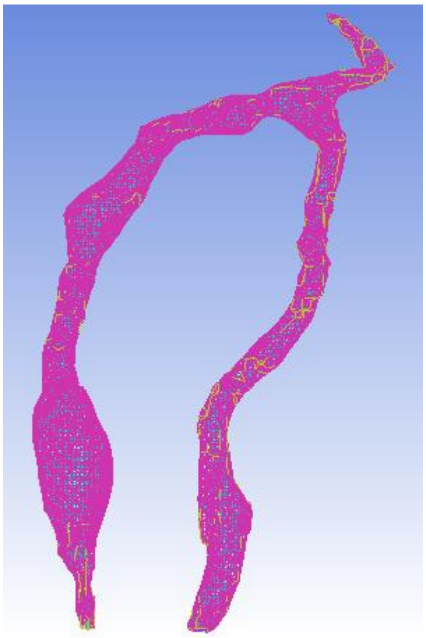

Figure 2. Tetrahedral mesh representation

2.3 Numerical model and flow conditaions

Mathematic governing equations for incompressible flow and according to the literature (Fox et al., 2006), are presented below:

Mass conservation equation:

$$\nabla \cdot \vec{V} = 0 \tag{1}$$

Momentum conservation equation:

$$\rho\left(\frac{D\vec{V}}{Dt}\right) = -\nabla p + \mu \nabla^2 \vec{V} \tag{2}$$

where ρ is the fluid density (kg/m³), $\vec{V}$ is the velocity vector (m/s), t is the time (s), p is the pressure (Pa) and μ is the dynamic fluid viscosity (Pa.s). The CFD code based on the finite volume method (Fluent 6.2.16 Academic License) was used in this study. Discretization of the governing equations at each control volume involved a first order upwind differencing scheme. The resulting system of algebraic equation was solved iteratively using a procedure based on the semi-implicit SIMPLE algorithm. In the AVF model, the inlet velocity profiles were maintained uniform across the inlet cross section. The outlet condition requires that velocity gradients in flow direction be zero. This condition is acceptable due to the outlet boundary having been located far downstream from the junction. The no slip condition was applied to all the walls. Fluid properties were assumed according to the literature (Berger et al., 1996): $\rho = 1050$ kg/m³ and $\mu = 3.45$ mPa.s. The unsteady flow condition the used velocity waveform is showed in the figure 3. The specific points I, II and III showed in the cycle (figure 3) are those used to plot the results.

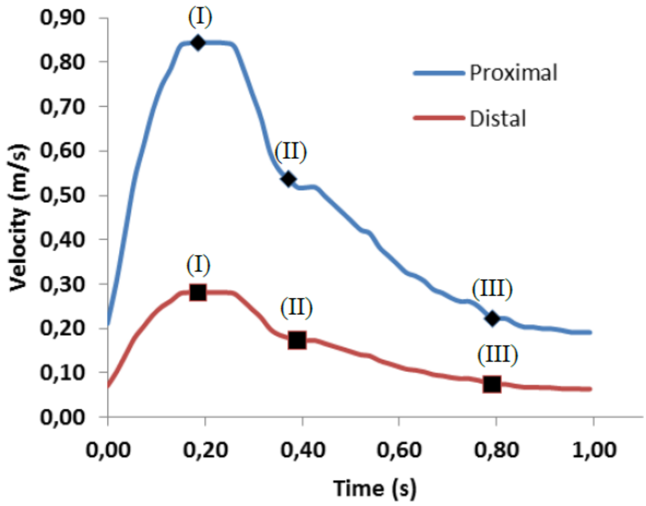

Figure 3. Velocity waveform obtained from intraoperative recording patients

3. RESULTS

The figure 4 shows the flow patterns at three specific points in the cycle. The proximal artery did not show recirculation, patterns are highly stable in the three points over the cicle. In the vein, nonuniform geometry of the vessel wall leads to intense recirculations. During the instant time I (systole), there was an important area of recirculation on the ascending side of the AVF, immediately after the anastomosis, the vortices appear and the helical movement in the vein appears in this time. In the instant time II (diastole), these recirculation and the helical movement are intensified, especially in the dilatation zones of the vein. In the instant time III (diastole), the recirculation in the anastomosis was decreased, the flow after the vein stenosis move initially in direction opposite to the main flow and then recirculate following the main bloodstream.

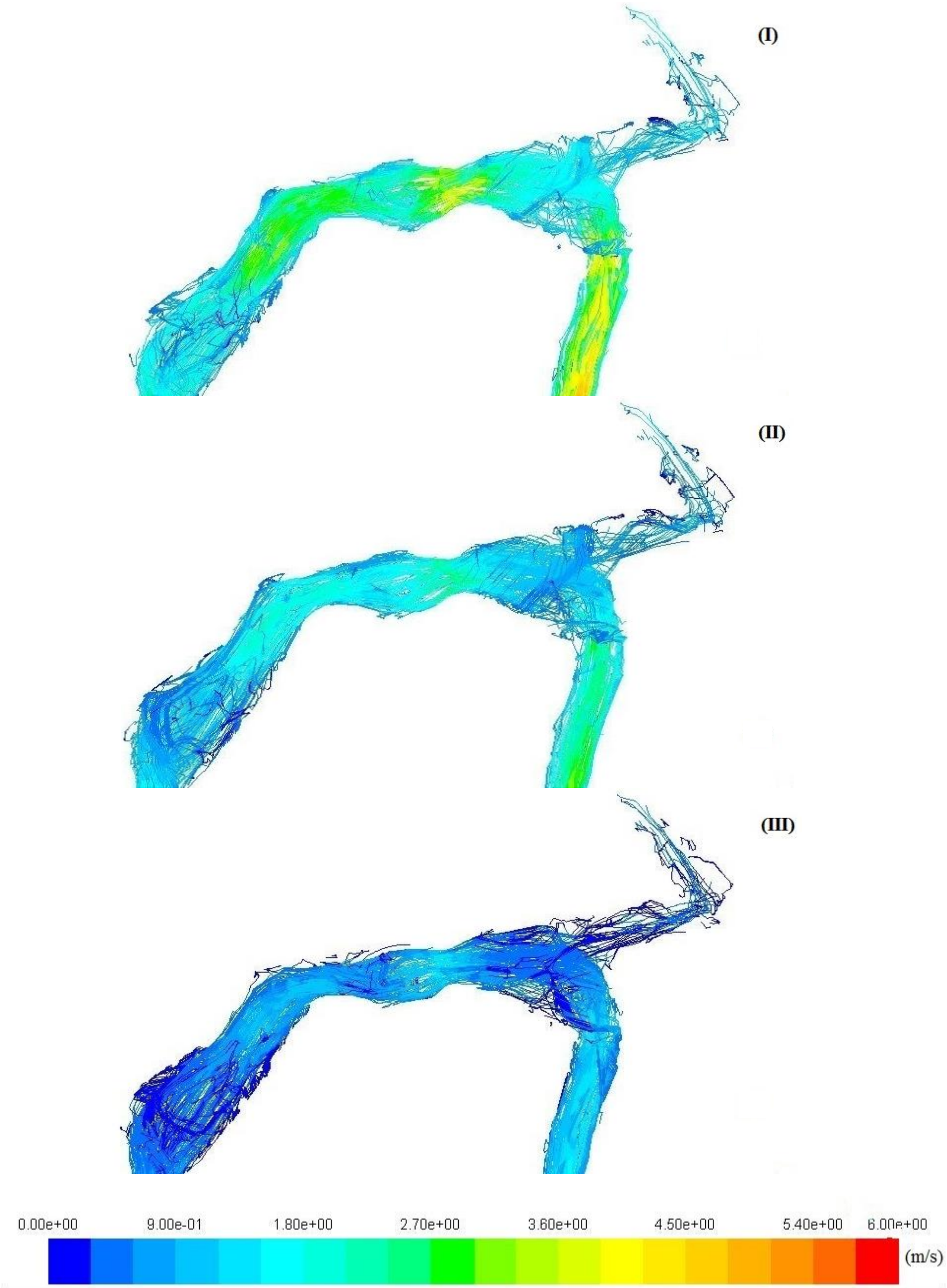

Figure 4. Pulsatile flow streamlines patterns at three specific points in the cycle

Figure 5 shows the wall shear stress distribution at three specific points in the cycle. In the cicle point I, the proximal artery presented the highest WSS in this analysis, the values were approximately 55 Pa, in the anastomosis inlet, WSS decreased to 16 Pa and increased in the stenosis, 4.95 Pa. In the point II, WSS presented a similar behavior, but with lowest values, the proximal artery showed 30 Pa of maximum value. In the cicle point III, WSS was very low, the proximal artery showed maximum value 8.50 Pa and in the other regions do not exceeds 5 Pa.

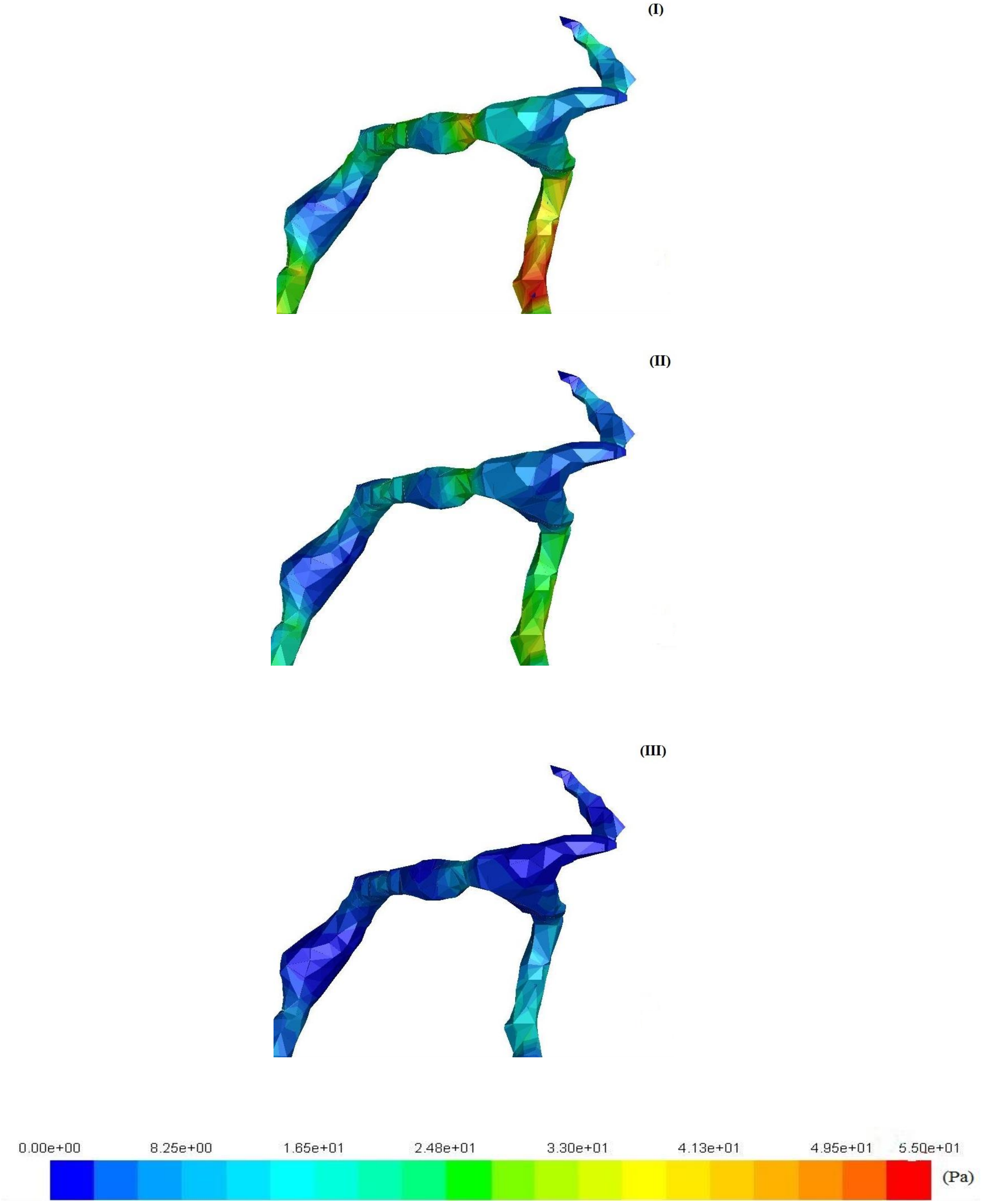

Figure 5. WSS at three specific points in the cycle

4. DISCUSSION

In this work, the flow visualization in AVF model was obtained through numerical simulation using Fluent 13. The three dimensional geometry of the AVF was built from tomography images of a patient. The objective was evaluate and quantify the blood flow patterns in mechanisms involved in failure of AVF for hemodialysis access. The limitations of our numerical analysis of blood flow is related to the assumption of rigid walls of the AVF and that was not possible use the data inlet parameters of the patient.

Flow disturbances and turbulence that may develop at the venous anastomosis of the AVF have also been documented to influence intimal–medial thickening (Fillinger et al., 1989) and endothelial cell turnover (Davies et al., 1986). It has been observed that when wall shear stress is low and oscillating, and there are zones of shear stress spatial gradients, vessel walls are more prone to vascular damage.

During the cardiac cycle, 1/3 of the time is attributed to the systolic phase and 2/3 to the diastolic phase. According to the results presented here, perturbation, recirculation and separation zones are intensified during the diastolic phase (Figures 4a and 4b). The flow in the anastomosis and the dilatation of the vein was turbulent and flow patterns that occur in those places were strictly connected with their geometrical shape. The nonuniform geometry of the anastomosis forces blood flow to change direction rapidly, this fact can explain the helicoidal movement in a few áreas. The anastomosis is considered to be a place of occurrence of clot risk because the blood velocity rapidly decreases and the blood flow can be even reversed locally. This clot could be transported for lower vessels and occlude them.

Fry (1968) had reported that the values of wall shear stress between 35 and 40 Pa can cause physical damage in endothelial cells within an hour of exposure. The proximal artery and the stenosis are áreas where the WSS were over 40 Pa in the systole phase (Figure 5a). Lower values of wall shear stress, below 1 Pa, have shown to be associated with the development of intimal hyperplasia in arterial anastomosis (Sallam et al., 1996). The distal artery and dilataions regions of the vein shows WSS values below 1 Pa in the point III of the cicle.

5. REFERENCES

Berger, S.A., W. Goldsmith, E.R. Lewis (1996), “Introduction to Bioengineering”, England: Oxford University Press.

Davies, P. F., Remuzzi, A., Gordon, E. J., Dewey, C. F., Jr., and Gimbrone, M. A., Jr., 1986, ‘‘Turbulent Fluid Shear Stress Induces Vascular Endothelial Cell Turnover in Vitro,’’ Proc. Natl. Acad. Sci. U.S.A., 83, pp. 2114–2117.

Fillinger, M. F., Reinitz, E. R., Schwartz, R. A., Resetarits, D. E., Paskanik, A. M., and Bredenberg, C. E., 1989, ‘‘Beneficial Effects of Banding on Venous Intimal-Medial Hyperplasia in Arteriovenous Loop Grafts,’’ Am. J. Surg., 158, No. 2, pp. 87–94.

Fox, R.W.; Mcdonald, A.T.; Pritchard, P.J. Introdução à mecânica dos fluidos. LTC editora, tradução para o português sexta edição, 798 p, 2006.

Fry, D.L. (1968), “Acute vascular endothelial changes associated with increased blood velocity gradients”, Circulation Research, 22, 165-197.

Sivanesan, S., How, T.V., Black, R.A. and Bakran, A., 1999. “Flow patterns in the radiocephalic arteriovenous fistula: an in vitro study”. Journal of Biomechanics, Vol. 32, No.9, pp. 915-925.

Van, T.I., De, W.D., Tordoir, J., Verdonck, P., 2005. “Hemodynamics and complications encountered with arteriovenous fistulas and grafts as vascular access for hemodialysis: a review”. Annals of Biomedical Engineering, Vol. 33, No. 9, pp. 1142–1157.

Wedgwood KR, Wiggins PA, Guillou PJ., 1984. “A prospective study of end-to-side vs. side-to-side arteriovenous fistulas for haemodialysis”. British Journal Surgery, Vol. 71, No. 8, pp. 640–642.

Yerdel, M. A., Kesenci, M., Yazicioglu, K. M., Do¨seyen, Z., Tu¨rkcapar, A. G., and Anadol, E., 1997. ‘‘Effect of Haemodynamic Variables on Surgically Created Arteriovenous Fistula Flow’’. Nephrology Dialysis Transplantation, Vol. 12, No. 8, pp. 1684–1688.